AD_____

Award Number: W81XWH-05-1-0367

TITLE: Systemic oncolytic cytokine HSV therapy of prostate cancer

PRINCIPAL INVESTIGATOR: Brent J. Passer, Ph.D.

CONTRACTING ORGANIZATION: Massachusetts General Hospital
Boston, MA 02114-2554

REPORT DATE: May 2008

TYPE OF REPORT: Final

PREPARED FOR: U.S. Army Medical Research and Materiel Command
Fort Detrick, Maryland 21702-5012

REPORT DOCUMENTATION PAGE

Form Approved
OMB No. 0704-0188

1. REPORT DATE	2. REPORT TYPE	3. DATES COVERED
14-05-2008	Final	15 APR 2005 - 14 APR 2008

4. TITLE AND SUBTITLE

Systemic oncolytic cytokine HSV therapy of prostate cancer

5a. CONTRACT NUMBER

5b. GRANT NUMBER
W81XWH-05-1-0367

5c. PROGRAM ELEMENT NUMBER

6. AUTHOR(S)

Brent J. Passer, Ph.D.

Email:

5d. PROJECT NUMBER

5e. TASK NUMBER

5f. WORK UNIT NUMBER

7. PERFORMING ORGANIZATION NAME(S) AND ADDRESS(ES)

Massachusetts General Hospital
Boston, MA 02114-2554

8. PERFORMING ORGANIZATION REPORT NUMBER

9. SPONSORING / MONITORING AGENCY NAME(S) AND ADDRESS(ES)
U.S. Army Medical Research and Materiel Command
Fort Detrick, Maryland 21702-5012

10. SPONSOR/MONITOR'S ACRONYM(S)

11. SPONSOR/MONITOR'S REPORT NUMBER(S)

12. DISTRIBUTION / AVAILABILITY STATEMENT
Approved for Public Release; Distribution Unlimited

13. SUPPLEMENTARY NOTES

14. ABSTRACT

The purpose of the present work is to evaluate the use of oncolytic HSV vectors (oHSV) and their cytokine-containing derivatives as potential therapeutic modalities in the transgenic TRAMP mouse, which recapitulates the developmental hallmarks in treating prostate cancer. We show that expression of interleukin 12 (IL-12) from NV1042 virus, a derivative of NV1023, was substantially effective at reducing the frequency of developing prostate cancer and lung metastases, even when the mice were treated after the onset of metastasis at 18 weeks of age. In October of 2007, we published this work in Cancer Research. Furthermore, we have extended these finding by using a novel complementary approach. Human prostate cancer tissues derived from radical prostatectomies were used in a organotypic culture system to further assess the efficacy of oncolytic HSV virotherapy. Our data shows that while G47Δ specifically targets epithelial cells but not the surrounding stroma, wild-type HSV is promiscuous in that it also infects prostate stroma. Lastly, G47Δ was shown to be more at least 10-fold more effective than G207, from which G47Δ was made, in its ability to replicate in these cancer specimens.

15. SUBJECT TERMS
Prostate cancer, Oncolytic HSV

16. SECURITY CLASSIFICATION OF:			17. LIMITATION OF ABSTRACT	18. NUMBER OF PAGES	19a. NAME OF RESPONSIBLE PERSON
a. REPORT	b. ABSTRACT	c. THIS PAGE			USAMRMC
U	U	U	UU	17	19b. TELEPHONE NUMBER *(include area code)*

Table of Contents

Page

Introduction……..…….…….. 3

Body…….. 3

Key Research Accomplishments…….…….. 7

Reportable Outcomes…… 8

Conclusion…… 8

References……. 8

Appendices…… 9

Systemic Oncolytic Cytokine HSV Therapy of Prostate Cancer

Final report August 2008 Brent J. Passer (PI)

INTRODUCTION

Oncolytic HSV-based vectors selectively replicate in tumor cells causing direct killing ie., oncolysis, while at the same time sparing normal cells. To better assess the utility of oncolytic HSV vectors in treating prostate cancer, we have taken advantage of a transgenic mouse model system called TRAMP, which develops prostate cancer spontaneously and closely mirrors the progression of prostate cancer seen in humans. Overall, we have accomplished the majority of goals as outlined by the three specific aims of this grant. A manuscript entitled, "Systemic therapy of spontaneous prostate cancer in transgenic mice with oncolytic herpes simplex viruses" by Varghese et al. has been recently published in *Cancer Research* (see attached manuscript in appendices). Moreover, we have made significant strides in assessing the use of organotypic cultures derived from human prostate cancer specimens to study oncolytic HSV spread and replication.

BODY

Overall, we have demonstrated that:

1. Inbred TRAMP mice displayed a consistent and predictable temporal pattern of prostate cancer progression, ie., low grade PIN (8 weeks) high grade PIN (10 weeks), prostate adenocarcinoma (12 weeks) and metastasis to the lungs (18 weeks). (**Aim 1**)
2. Systemic delivery of oncolytic NV1042 (expressing IL-12) replicates within prostate tumors as defined by β-gal staining and quantitative PCR of HSV gB sequence. (**Aim 2**)
3. Oncolytic NV1023 and to a greater extent NV1042 vectors delivered systemically at 12 weeks of age promoted robust regression of prostate tumor growth by 24 weeks of age. (**Aim 2**)
4. NV1042 also diminished prostate tumor size even when delivered by 18 weeks of age (period of metastasis). (**Aim 3**)
5. A significant reduction in the frequency of metastasis to the peri-aortic lymph nodes after administration of either NV1023 or NV1042 (Mock 86% as compared to NV1023 (14%) and NV1042 (25%). (**Aim 3**).
6. A tendency toward a reduction of metastasis to the lungs by NV1042 and NV1023 treatments. Although this was not statistically significant. (**Aim 3**).
7. NV1042 persistence within the tumor as defined by β-gal staining is different from senescence-associated β-gal activity, which can arise in prostate hyperplasia. (**Aim 2**).
8. NV1042 persistence within the tumor as defined by β-gal staining is different from senescence-associated β-gal activity, which can arise in prostate hyperplasia. (**Aim 2**).
9. Verifying by immunohistochemistry that anti-β-gal staining mirrored X-gal staining. (**Aim 2**).

Recently, we noted major inconsistencies in prostate tumor sizes in TRAMP mice in untreated mice at 24 weeks of age. This makes interpretation of treatment conditions difficult and we are currently trying to rectify this problem. While we believe that we have

made major strides in better characterizing the utility of oHSV for prostate cancer in this transgenic model system, the lack of consistent tumor size has hampered ongoing and future-planned studies. We have continued to breed these mice in order to obtain consistent tumor sizes. In addition, we will continue to seek the expertise of our collaborator Dr. Petur Nielsen, a MGH pathologist.

As discussed in last years progress report, we have also developed a novel complementary approach towards assessing the effectiveness of oncolytic HSV therapy in prostate cancer (not in the grant application but highly relevant). This experimental paradigm takes advantage of previously published work in which human prostate cancer biopsies can be easily maintained *in vitro* on a collagen sponge for 1-2 weeks (Nevalainen *et al*, 1993). The advantages of prostate tumor organ cultures are: (1) use of primary human prostate cancer biopsy material (as opposed to passaged prostate cancer cell cultures); (2) the three-dimensional structure remains intact (in contrast to typical monolayer cultures); (3) contains all the cell types present in the tumor; (4) contains 'normal' tissue/glands; (5) contains tumor foci at different stages of tumor progression; and (6) represents the genetic heterogeneity present within and between patients. Thus, factors that may affect viral entry and replication including cell-cell interactions and cell-matrix interactions remain preserved in this 3-dimensional milieu. Moreover, differences between prostate cancer cells, normal prostate gland cells, and interstitial cells can be explored. Human prostate cancer specimens are obtained from Surgical Pathology, immediately transported to the laboratory, cut into 2-4 mm^3 pieces, incubated with oHSV, and placed on semi-submersed collagen sponges in media (with or without) compound, where they remain viable for over 7 days (**Figure 1**). Eight to twelve samples can be obtained from a single specimen so that each treatment group contains multiple individual fragments and different treatment groups from a single patient.

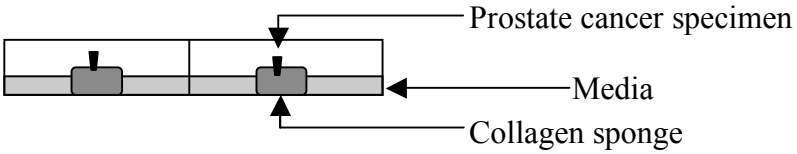

Figure 1. Prostate organ culture. Side-view of a 6-well plate containing prostate tumor fragments placed on a collagen sponge after being incubated with oncolytic HSV.

As nectin-1 is one of the major entry receptors for HSV infection, we assess the tissue distribution of nectin-1 expression in these surgical specimens. IHC analysis clearly shows strong anti-nectin-1 staining on the epithelial cells in the prostate (**Figure 2**). These data suggest that oncolytic HSV's likely infects the prostate epithelium via nectin-1 receptors. Furthermore, we have compared tropism of G47Δ with that of the wild-type HSV strain F, from which G47d was derived in these prostate explants.

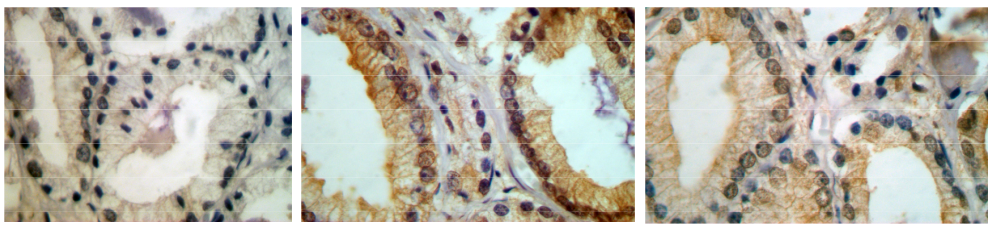

Neg. Control anti-nectin-1

Figure 2. Human prostate cancer specimens express the HSV entry receptor nectin-1. Prostate specimens sections where either stained with a rabbit serum (Neg. Control) or the rabbit anti-nectin-1 antibody (R166; gift from Dr. Claude Krummenacher, Univ. of Pennsylvania). Thereafter, tissues were incubated with an anti-rabbit secondary antibody conjugated to horseradish peroxidase and followed by to reveal the expression of nectin-1. Note that the majority of nectin-1 staining appears located on the epithelial cells. (50x)

Analysis of prostate specimens infected with G47Δ at days 3 and 5 post-infection by either X-gal staining (*ICP6* gene has been replaced by *LacZ*) or by immunostaining with anti-HSV glycoprotein C (gC) antibody shows that G47Δ specifically targets the epithelia of the prostatic ducts but spares the surrounding stroma. This was confirmed by immunostaining serial sections with cytokeratin 18, which specifically stains epithelial cells (**Figure 3A**). By d5, these ducts appeared extensively damaged presumably due to the oncolytic activity of G47Δ. While G47Δ appears restrictive in its pattern of infectivity and spread, ie.,prostate epithelial cells, anti-gC staining on tissues infected with wild-type strain F showed staining not only of epithelia but also the surrounding stroma (**Figure 3B**). This analysis demonstrates that wild-type HSV is promiscuous in nature to infect and spread in the in human prostate tissue.

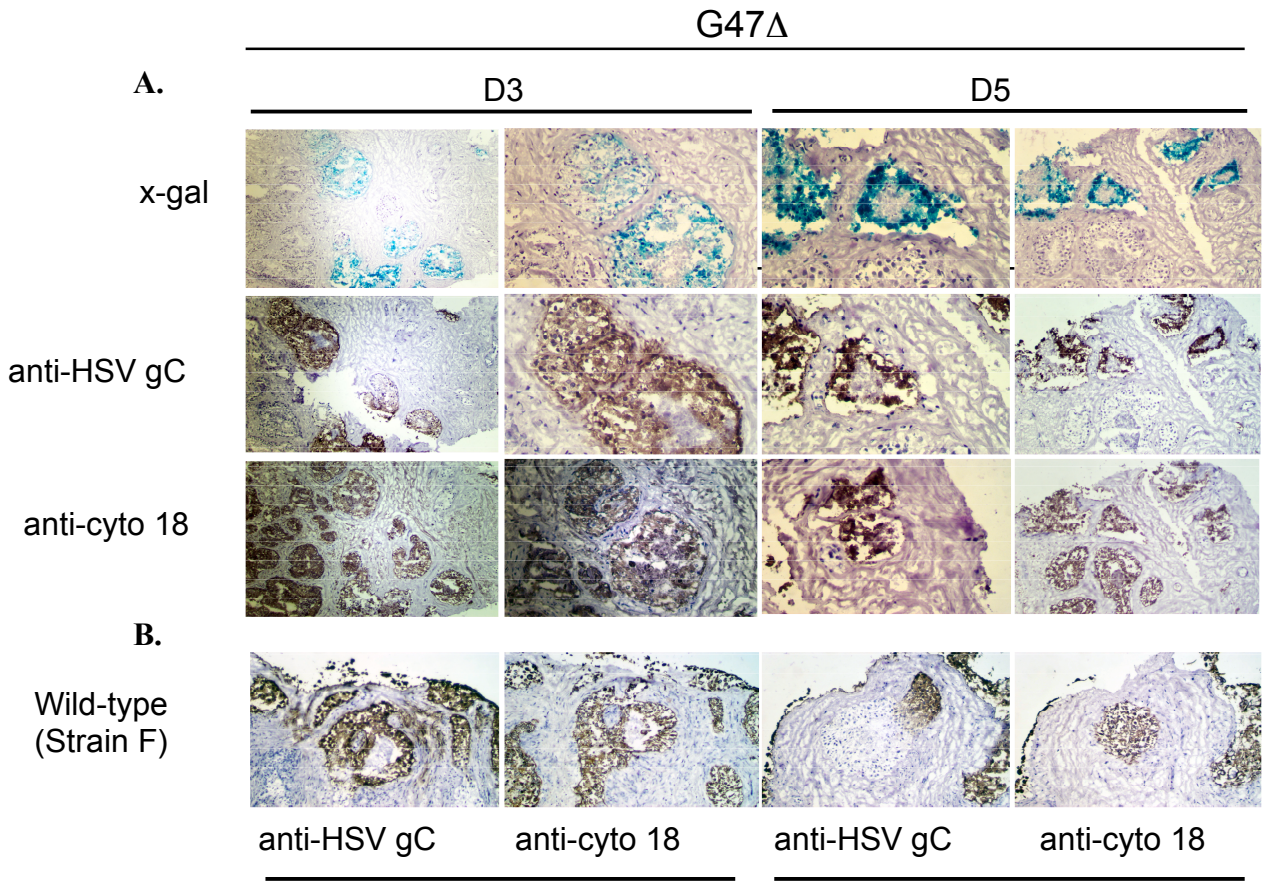

Figure 3. Oncolytic G47Δ specifically targets the prostatic ducts of human prostate cancer biopsies. (A) Prostate cancer specimens were treated with G47Δ and day 3 and 5 post-infection, tissues were fixed and sectioned. Tissues sections were stained with X-gal (blue) or stained with the anti-HSV glycoprotein C (gC) antibody. In addition, serial

sections were immunostained with anti-cytokeratin18 (brown) to demarcate the prostate epithelial cells within the ducts and to demonstrate that G47Δ infection overlaps with cytokeratin 18-expressing cells. Tissues sections were also counterstained with hematoxylin. Note the cauterized-like appearance of the prostatic ducts at D5 and the lack of B-gal^{+} cells in the surrounding stroma. (B) Similar experiments were performed with wild-type Strain F and serial sections were stained with either anti-HSV gC (left and middle right panels) and anti-cytokeratin 18 (middle left and right panels). Note that HSV gC expression is also found in cyto18-negative areas.

Finally, we also compared the replication capacity of oncolytic G47Δ, G207 as well as wild-type strain F in these organ cultures (**Figure 4**). G47Δ is derived from G207 by a deletion within the nonessential *α47* gene. Because of the overlapping transcripts encoding ICP47 and US11, the deletion in *α47* also places the late *US11* gene under control of the immediate-early *α47* promoter. This alteration of *US11* expression enhances the growth of *γ34.5* $^{-}$ mutants by precluding the shutoff of protein synthesis (Todo *et al*., 2001). To this end, tissues were infected with one of the three viruses (1-2x10^{6} pfu) and 5 days post-infection, tissues derived from these cancer specimens (n=6) were titered on Vero cells. This analysis shows that G47Δ was at least $\log_{10}$ more effective that G207. By contrast, strain F was more robust than either one of these vectors in its ability to replicate in these prostate tissues.

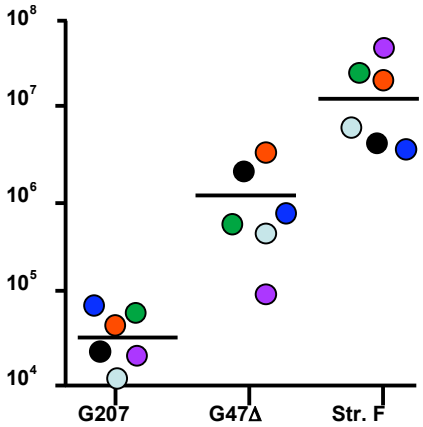

Figure 4. Oncolytic HSV's replicates in prostate organ cultures. At 5 days post-infection, organ cultures were removed from the collagen-sponge, extensively homogenized and titered onto Vero cells. The vertical axis is in pfu/mg human prostate tissue. Each color dot indicates a different prostate surgical specimen which was separately infected with one of the three indicated viruses (n=6). Although viral input ranged from ~30,000-100,000 pfu/mg of prostate tissue, the actual infectivity by oHSV is likely to be much less.

KEY RESEARCH ACCOMPLISHMENTS

- Addressed key questions from all three specific aims.
- Manuscript to *Cancer Research* has been published
- Reported on a novel complementary approach towards addressing the effectiveness and specificity of oncolytic HSV vectors in prostate cancer.

REPORTABLE OUTCOMES

1. Varghese S, Rabkin SD, Nielsen GP, MacGarvey U, Liu R, Martuza RL. Systemic therapy of spontaneous prostate cancer in transgenic mice with oncolytic herpes simplex viruses. Cancer Res. 2007, 67:9371-9.

CONCLUSIONS

In conclusion, we demonstrated that systemic administration of oncolytic HSVs, in particular the IL-12 expressing NV1042 virus, is effective against primary prostate tumors as well as metastatic tumors independent of their location. These desirable therapeutic features of NV1042 render it a highly valuable agent either as a primary treatment option or as an adjuvant approach following surgery to eliminate micrometastases.

REFERENCES

Nevalainen MT, Harkonen PL, Valve EM, Ping W, Nurmi M, Martikainen PM. Hormon. regulation of human prostate in organ culture. Cancer Res. 1993. 53:5199-207.

Todo T, Martuza RL, Rabkin SD, Johnson PAOncolytic herpes simplex virus vector with enhanced MHC class I presentation and tumor cell killing. Proc Natl Acad Sci U S A. 2001, 98:6396-401.

APPENDICES

See accompanied manuscript

Systemic Therapy of Spontaneous Prostate Cancer in Transgenic Mice with Oncolytic Herpes Simplex Viruses

Susan Varghese,[1,2] Samuel D. Rabkin,[1,2] G. Petur Nielsen,[3] Usha MacGarvey,[1] Renbin Liu,[1,2] and Robert L. Martuza[1,2]

[1]Department of Neurosurgery, Massachusetts General Hospital; [2]Department of Surgery (Neurosurgery), Harvard Medical School; and [3]Department of Pathology, Massachusetts General Hospital and Harvard Medical School, Boston, Massachusetts

Abstract

Oncolytic viruses are an innovative therapeutic strategy for cancer, wherein viral replication and cytotoxicity are selective for tumor cells. Here we show the efficacy of systemically administered oncolytic viruses for the treatment of spontaneously arising tumors, specifically the use of oncolytic herpes simplex viruses (HSV) administered i.v. to treat spontaneously developing primary and metastatic prostate cancer in the transgenic TRAMP mouse, which recapitulates human prostate cancer progression. Four administrations of systemically delivered NV1023 virus, an HSV-1/HSV-2 oncolytic recombinant, to TRAMP mice at 12 or 18 weeks of age (presence of prostate adenocarcinoma or metastatic disease, respectively) inhibited primary tumor growth and metastases to lymph nodes. Expression of interleukin 12 (IL-12) from NV1042 virus, a derivative of NV1023, was additionally effective, significantly reducing the frequency of development of prostate cancer and lung metastases, even when the mice were treated after the onset of metastasis at 18 weeks of age. NV1042-infected cells, as detected by 5-bromo-4-chloro-3-indolyl-β-D-galactopyranoside staining for *Lac Z* expressed by the virus, were present in prostate tumors 1 week after the final virus injection and viral DNA was detected at 2 weeks after final virus injection by real-time PCR in primary and metastatic tumors but not in liver or blood. No toxicity was observed in any of the treated mice. The efficacy of the IL-12–expressing NV1042 virus in this aggressive prostate cancer model using a clinically relevant treatment paradigm merits its consideration for clinical studies. [Cancer Res 2007;67(19):9371–9]

Introduction

Oncolytic viruses designed to differentially target cancer cells while sparing normal tissues have advanced in the past decade to the forefront of innovative strategies for cancer treatment (1, 2). Since the conception in 1991 of using mutated herpes simplex virus (HSV), a neurotropic virus, to treat brain tumors (3), the unique biology of HSV coupled with genetic manipulation techniques has greatly aided in the development of more potent HSV vectors while conferring safety and specificity (4). Currently, four oncolytic HSV vectors, G207, HSV 1716, NV1020, and Oncovex$^{GM\text{-}CSF}$, delivered intracerebrally, intraneoplastically, or intra-arterially, have successfully completed phase I clinical trials (4–6). These and other oncolytic HSVs have been efficacious in treating a variety of cancers in animal models (4, 7). In addition to their direct tumoricidal effect, oncolytic herpes viruses are also capable of eliciting an antitumor immune response (8–10), an important feature when treating metastatic tumors, especially those that are clinically occult.

Accumulating evidence suggests that oncolytic HSVs are potentially useful for treating prostate cancer: (*a*) G207, a multimutated herpes simplex virus-1 (HSV-1; ref. 11), is safe when administered into the prostate in preclinical animal models, and is a nerve-sparing virus (12, 13). This overcomes a current challenge of conventional treatments such as surgery and radiation therapy, which are associated with risks of nerve damage. (*b*) Oncolytic HSV mutants, including G207 and NV1020, have shown efficacy against human prostate cancer xenografts and mouse prostate cancers following intraneoplastic or i.v. administration (14–17). (*c*) G207 and other vectors are effective against human prostate cancer irrespective of hormone status or radiosensitivity (14, 16, 18)—a major advantage in its application for advanced forms of the disease in which hormone- and radiation-refractory tumor is an inevitable progression.

To date, however, all efficacy studies with HSV vectors for prostate cancer have used implanted tumor models, which are artificial systems with respect to their milieu and lymphovascular supply. Whereas these implanted models are easily amenable to therapeutic manipulation, they do not truly reflect the *in situ* cancer situation and may affect the outcome of the therapy being investigated. Genetically engineered mouse models that develop prostate cancer spontaneously are currently the most representative models to conduct efficacy studies. Therefore, we have used the transgenic TRAMP mouse, which develops prostate cancer spontaneously with progression to metastatic disease (19, 20). In TRAMP mice, the rat probasin promoter regulated by androgens drives SV40 T antigen expression, restricting its expression to epithelial cells of the prostate. Histologic progression of prostate cancer in TRAMP mice closely recapitulates that of humans, with the development of prostatic intraepithelial neoplasia (PIN) by 8 weeks of age, prostate carcinoma by 12 weeks, and metastatic cancer in periaortic lymph node and lungs by 18 weeks of age (20).

As a prelude to the studies in TRAMP mice, we examined the efficacy of G207, NV1023, and NV1042 against s.c. and metastatic lung tumors using the TRAMP-C2 prostate cancer cell line, which was established from a spontaneously occurring prostate adenocarcinoma of a TRAMP mouse (19). NV1023 is derived from NV1020, which has been in clinical trial for metastatic colon cancer to the liver and has deletions of one copy of *γ34.5,* the internal repeat, and *UL24* and *UL56* genes, as well as the addition of *gJ, gG, US2,* and *US3* genes from HSV-2 (21, 22). NV1023 has an additional

Note: S.D. Rabkin and G.P. Nielsen contributed equally to this work. Current address for R. Liu: The First Affiliated Hospital, Sun Yat-Sen University, Guangzhou, P.R. China.

Requests for reprints: Robert L. Martuza, Department of Neurosurgery, Massachusetts General Hospital, WHT-502, 55 Fruit Street, Boston, MA 02114. Phone: 617-726-8581; Fax: 617-726-4814; E-mail: rmartuza@partners.org.

doi:10.1158/0008-5472.CAN-07-0674

insertion of *LacZ* and deletion of *ICP47, US11,* and *US10* genes (21). Comparison of efficacy in s.c. or metastatic lung TRAMP-C2 tumors showed that the murine interleukin 12 (IL-12)–expressing NV1042 virus was superior to its parent, NV1023, and G207 (17, 23). We also showed that IL-12 expression from NV1042 resulted in both immune and antiangiogenic effects (17, 23).

Based on the above findings, we investigated the utility of systemically administered NV1023 and NV1042 to treat spontaneously arising prostate cancer and metastasis in TRAMP mice. Results show that both NV1023 and NV1042 significantly inhibited the growth of primary tumors in prostate and metastasis in periaortic lymph nodes. NV1042 was additionally effective in reducing the frequency of the development of prostate carcinoma and lung metastasis.

Materials and Methods

Mice. TRAMP (C57Bl/6 background) breeder pairs (female TRAMP and male C57Bl/6) were purchased from The Jackson Laboratory and bred in-house at the Center for Comparative Medicine facility at Massachusetts General Hospital. Female transgenic F_1 pups were crossed with male FVB/N mice obtained from National Cancer Institute to generate TRAMP mice on an FVB/N background. The pups were genotyped at 3 weeks of age using SV40 large T antigen primers (5′-CAGAGCAGAATTGTGGAGTGG-3′ and 5′-ACAAACCACAACTAGAATGCAGTG-3′) for PCR of tail genomic DNA isolated using phenol-chloroform extraction (24). F_1 male TRAMP mice obtained from this cross-breeding were used for all experiments described below. Mice were housed in a pathogen-free facility and all animal procedures were conducted with approval from Massachusetts General Hospital Subcommittee on Research Animal Care. All animal studies were blinded.

Viruses. Purified virus stocks of NV1023 and NV1042 were obtained from MediGene, Inc. Construction of NV1023 and NV1042 has previously been described (21). NV1023, derived from NV1020 (R7020), a HSV-1/HSV-2 intertypic recombinant developed as a vaccine strain (22), contains an insertion of *LacZ* into the *ICP47* locus, deleting *ICP47, US11,* and *US10* (21). NV1042 is NV1023 with an insertion of murine IL-12 cDNA (p35 and p40 as a single polypeptide separated by elastin motifs) expressed from a hybrid α4-TK promoter (21). The viruses were individually titered on Vero (African green monkey kidney) cells by plaque assay. NV1042-infected TRAMP-C2 cells secreted 52 ng/mL of IL-12 (17).

Virus treatment and efficacy evaluation. Twelve-week-old (n = 8–9 per group) or 18-week-old (n = 17 per group) male TRAMP mice were inoculated via tail vein with 2×10^7 plaque-forming units (pfu) of NV1023 or NV1042 or virus buffer consisting of 10% glycerol in PBS (mock) in a 200-μL volume on days 0, 3, 7, and 10. By day 14 after initiation of treatment, anti-HSV serum antibody was detectable (data not shown). Mice were monitored biweekly and sacrificed if morbid. At 24 weeks, all mice were sacrificed, terminating the experiment. Prostate and seminal vesicles were removed en bloc, weighed, and photographed. Formalin-fixed sections of prostate, periaortic lymph nodes, and lungs were evaluated by H&E staining and the frequency of carcinoma was scored in a blinded manner by the collaborating pathologist (G.P.N.). Histologic grading of prostate samples was done as previously published (25).

Virus biodistribution studies. TRAMP mice were treated with 2×10^7 pfu of NV1042 on days 0, 3, 7, and 10. Mice were sacrificed at predetermined days and various tissues were evaluated for *β-galactosidase* by 5-bromo-4-chloro-3-indolyl-β-D-galactopyranoside (X-gal) staining and immunohistochemistry and for the presence of HSV-1 DNA by real-time PCR.

***β-Galactosidase* staining.** Tissue cryostat sections of prostate and seminal vesicles, periaortic lymph nodes, lung, liver, and brain obtained from three mice each sacrificed on days 11, 13, and 17 (or 1, 3, and 7 days after the final treatment) were analyzed by X-gal staining at pH 7.2, as previously described. For senescence-associated β-galactosidase staining, we carried out X-gal histochemistry at pH 6.0 (26). Sections were counterstained with eosin or H&E. For immunohistochemistry, sections were washed with 0.2% Triton X-100 in PBS, 0.3% hydrogen peroxide in PBS, 1% and then 10% goat serum in PBS; incubated with rabbit anti–*E. coli* β-galactosidase (1:1,000; Abcam, Inc.) overnight at 4°C; washed in PBS; and incubated with biotinylated goat anti-rabbit immunoglobulin G (Vector Laboratories). Immunoreactive material was detected with Vectastain Elite ABC and diaminobenzidine kits (Vector Laboratories).

Real-time PCR. NV1042-treated mice were sacrificed on days 11, 13, and 24 (or 1, 3, and 14 days after the final treatment) and various tissues (prostate and seminal vesicles, periaortic lymph nodes, lung, liver, brain, and blood) were removed aseptically and immediately snap frozen on dry ice with isopentane. Tissues were resuspended in nucleic acid lysis buffer (Applied Biosystems) and homogenized using a Mixer Mill (Qiagen). Total DNA was extracted from the homogenate using ABI Prism 6100 Nucleic Acid PrepStation (Applied Biosystems). Absolute quantification of viral DNA was conducted by real-time TaqMan PCR using HSV-1 *gB* primer sequences (forward primer, 5′-TGTGTACATGTCCCCGTTTTACG-3′; reverse primer, 5′-GCGTAGAAGCCGTCAACCT-3′; probe, 5′-ACACCAGCTACGCCGCC-3′) synthesized using Assays-by-Design service (Applied Biosystems). Mouse glyceraldehyde-3-phosphate dehydrogenase (GAPDH) primers (Applied Biosystems) were used as endogenous control for input DNA. Strain F genomic DNA served as positive control and was used to generate a standard curve from 15 to 2.4×10^5 copies.

Statistical analysis. Statistical analyses were conducted by comparing NV1023- or NV1042-treated mice groups with mock, or NV1023-treated with NV1042-treated mice group. Because the experimental data of prostate tumor weight from the efficacy studies did not follow a normal Gaussian distribution, nonparametric Mann-Whitney tests (two-tailed) were used to analyze significance between treatment groups. The frequency of carcinoma in prostate, periaortic lymph node, and lungs between treatment groups was conducted by contingency analysis using Fisher's exact two-sided test. Kaplan-Meier survival data were analyzed using χ^2 log-rank test. α levels for all analyses were $P < 0.05$; n values and exact P values are indicated in the text and legends. All statistical analyses were done using GraphPad Prism v.4.

Results

Spontaneous primary and metastatic prostate cancer development. Because the TRAMP mice were bred in-house, we determined the time line of prostate cancer and metastasis development before using them in viral therapy studies by analyzing 125 male transgenic TRAMP mice, and observed reproducibility with tumor development and progression. As illustrated in Fig. 1, TRAMP mice on the FVB/N background display PIN by 8 weeks of age, which progresses to carcinoma by 12 weeks and to metastases in periaortic lymph nodes and lung by 18 weeks of age. For comparison, histology of normal prostate from a nontransgenic littermate is shown. Systemic treatment with NV1023 or NV1042 was initiated at an age when mice first exhibit either primary prostate carcinoma (12 weeks) or metastasis (18 weeks). The mice were sacrificed at 24 weeks of age when untreated mice become moribund from disease.

Efficacy of systemic oncolytic HSV therapy on primary prostate cancer. Mouse cells are more resistant to HSV infection, and in our prior studies with implanted mouse prostate TRAMP-C2 cells in C57Bl/6 mice, we had noted that four intraneoplastic injections were significantly more effective than two treatments (17). Additionally, with TRAMP-C2 tumors metastatic to lung, we had observed that four i.v. administrations were significantly effective in inhibiting the growth of the tumors. Therefore, in this study using the spontaneous tumor model, four doses of 2×10^7 pfu of NV1023 or NV1042, or virus buffer, were administered i.v. on days 0, 3, 7, and 10 to 12-week-old TRAMP mice (n = 8–9 per group). The results show a substantial inhibition of primary

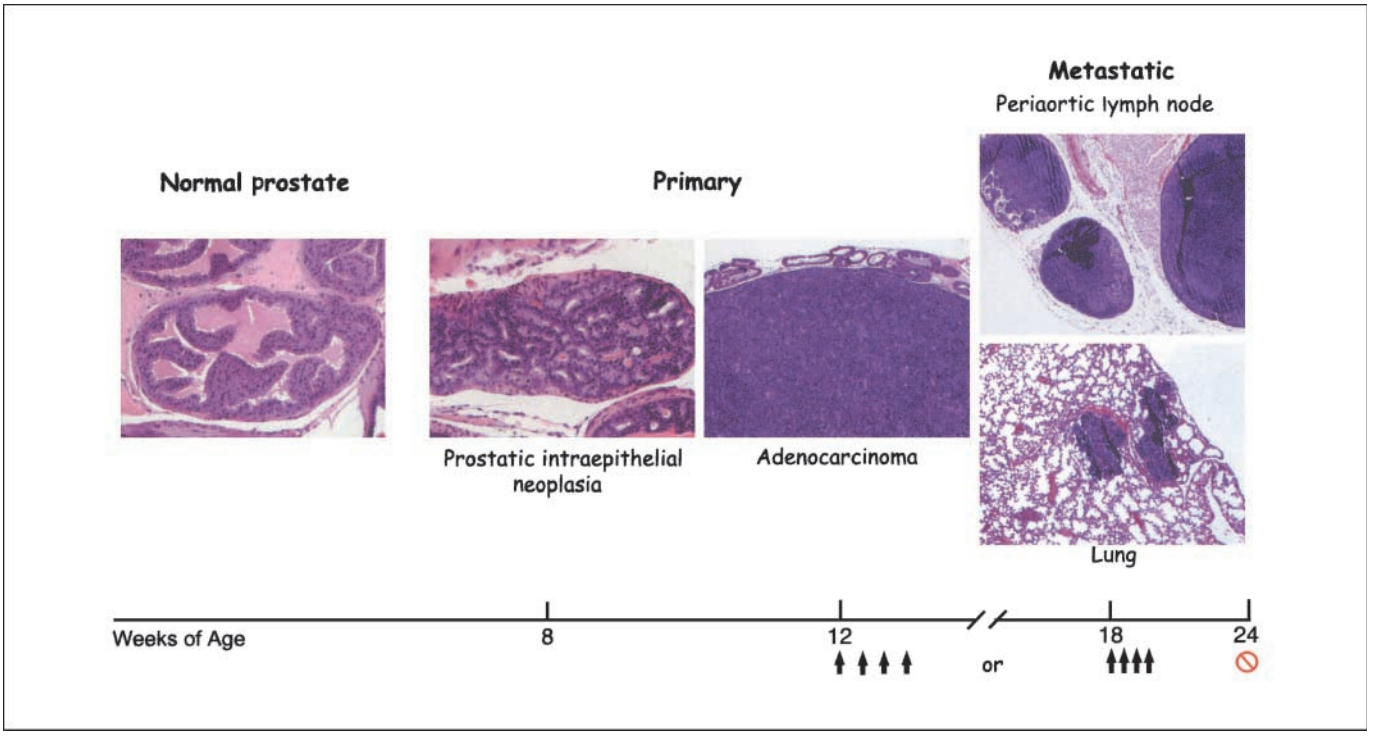

Figure 1. Spontaneous primary and metastatic prostate cancer development in TRAMP mice. A normal prostate gland from a nontransgenic male littermate (*left*). Time line of primary prostate and metastatic cancer development in TRAMP mice starting at 8 wk of age when they develop PIN, progressing to invasive adenocarcinoma by 12 wk of age. Metastasis in periaortic lymph node and lung are observed by 18 wk of age.

prostate cancer growth in virus-treated mice when compared with mock mice as illustrated in the gross photograph (Fig. 2*A*). Because multifocal tumors also arise in the seminal vesicles of these mice and often coalesce with the prostate gland by sacrifice (24 weeks), the carcinomatous mass containing both prostate and seminal vesicles was excised as one unit and weighed. Distribution of prostate and seminal vesicle tumor weights (Fig. 2*B*) illustrates that mock-treated mice harbored tumors with a mean weight of 10.17 g, NV1023 with 3.98 g ($P = 0.026$, versus mock, Mann-Whitney test), and NV1042 with 2.79 g ($P = 0.003$, versus mock, Mann-Whitney test). For comparative purposes, the average weight of prostate and seminal vesicles from nontransgenic TRAMP mice is 0.78 g. In this experiment, two of nine mice from both the mock- and NV1023-treated groups died within 2 days of the 24-week sacrifice and one mouse from the NV1042 group died 1 week after treatment (at $\sim$14 weeks of age). Histologic analysis of prostates from these dead mice showed that those from the mock and NV1023 treatment groups had large prostate tumors comprising of carcinoma, whereas the single NV1042-treated mouse did not display any evidence of cancer and therefore likely died from unrelated causes. H&E analysis of prostates showed consistent histologic grades among the treatment groups and included glands with normal histology, PIN, and invasive carcinoma of undifferentiated type. Whereas 8 of 9 (89%) mock mice had progressed to undifferentiated invasive carcinoma, only 6 of 9 (67%) NV1023-treated and 2 of 8 (25%) NV1042-treated mice ($P = 0.015$, versus mock, Fisher's exact test) progressed to invasive carcinoma (Table 1). Correspondingly, PIN was the highest grade observed in the prostates of 3 of 9 (33%) NV0123-treated and 5 of 8 (63%) NV1042-treated mice, suggesting an inhibition of tumor progression in these treated mice. Thus, whereas both NV1023 and NV1042 were equally effective in inhibiting the growth of primary tumors (as assessed by tumor weight) when treated at 12 weeks, only NV1042 was effective in inhibiting tumor progression (as assessed by histologic grading) compared with mock or NV1023. Representative H&E-stained prostates, based on the most frequently observed histologic stage, from various treatment groups are illustrated in Fig. 2*C*. The largest tumors were highly necrotic (seen as pink areas in Fig. 2*C*, mock) with islands of tumor cells closely apposed to blood vessels within the necrotic areas.

Both NV1023 and NV1042 also inhibited primary prostate tumor growth as compared with mock treatment in mice treated at 18 weeks of age ($n = 17$ per group), when they begin to exhibit metastasis (Fig. 3*A*). There was a significant difference in the number of animals surviving to 24 weeks, with 8 of 17 mock dying or being sacrificed between 22 and 24 weeks due to tumor burden, as compared with 3 of 17 NV1023 and 2 of 17 NV1042 ($P = 0.03$, NV1042 versus mock, χ^2 log-rank test). All of these mice harbored carcinoma within the prostate as determined by histologic analysis. Comparison of prostate and seminal vesicles weights in mice sacrificed at 24 weeks (Fig. 3*B*) shows a mean weight of 12.25 g in mock versus 6.54 g in NV1023 ($P = 0.04$ versus mock; Mann-Whitney test) and 3.66 g in NV1042 ($P = 0.002$, versus mock, Mann-Whitney test). Histologic analysis revealed that 16 of 17 (94%) mock mice, 13 of 17 (76%) of NV1023, and 10 of 17 (59%) of NV1042 ($P = 0.039$, versus mock, Fisher's exact test) harbored invasive carcinoma, which were either well-differentiated adenocarcinoma or undifferentiated carcinoma (Table 1). Treatment at 18 weeks of age also resulted in inhibition of tumor progression within the prostate gland, with 35% of NV1042-treated mice displaying PIN as the highest grade without any advancement to carcinoma. Thus, when treated at 12 or 18 weeks, only NV1042 was effective in

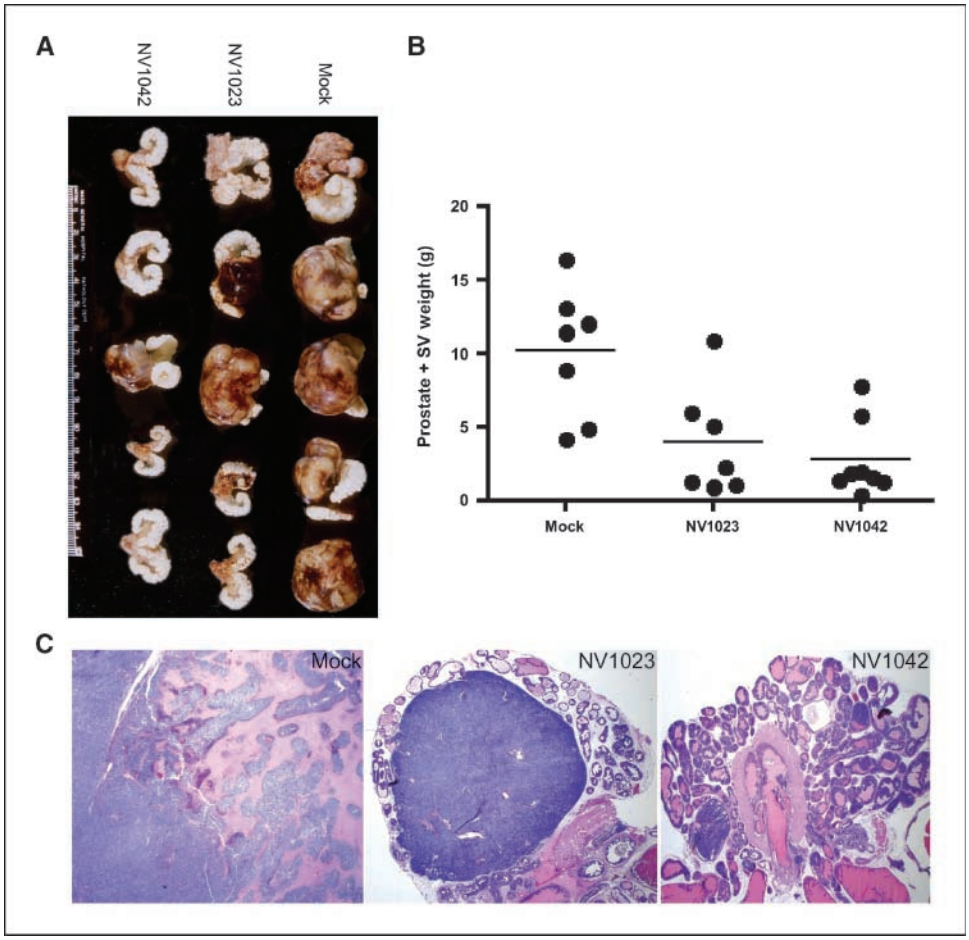

Figure 2. Efficacy of systemic oncolytic virus in TRAMP mice treated at 12 wk of age. *A,* photograph of representative prostate and seminal vesicles excised en bloc from various treatment groups illustrating prostate tumors. *B,* distribution of weights of prostate and seminal vesicles (*SV*) from mock (n = 7), NV1023 (n = 7), and NV1042 (n = 8). Mean is denoted by the line; mean weight ± SE for each group are as follows: mock, 10.17 ± 1.68 g; NV1023, 3.98 ± 1.39 g (P = 0.026, versus mock, Mann-Whitney test); NV1042, 2.79 ± 0.91g (P = 0.0037, versus mock, Mann-Whitney test). Mice dying before week 24 were not included in the analysis. *C,* H&E staining of prostates from mock-treated, which shows larger areas of necrosis, NV1023-treated, and NV1042-treated mice.

inhibiting tumor growth within the prostate (as measured by prostate weight) and development of invasive carcinoma (as assessed by histologic grading).

Efficacy of systemic oncolytic HSV therapy on metastasis. Treatment of TRAMP mice with NV1023 or NV1042 at 12 weeks of age, when they begin to develop prostate carcinoma, resulted in a significant reduction of metastatic frequency in periaortic lymph nodes from 86% in mock-treated to 14% in NV1023-treated mice (P = 0.03, versus mock, Fisher's exact test) and to 25% in NV1042 (P = 0.04, versus mock, Fisher's exact test). Whereas there was a

Table 1. Frequency of prostate lesions and metastatic cancer in TRAMP mice treated with oncolytic HSVs

Site/histology	Treatment at 12 wk of age, n (%)			Treatment at 18 wk of age, n (%)		
	Mock (n = 7s + 2d)	NV1023 (n = 7s + 2d)	NV1042 (n = 8s)	Mock (n = 9s + 8d)	NV1023 (n = 14s + 3d)	NV1042 (n = 15s + 2d)
Prostate—normal			1/8 (12.5)			1/17 (6)
Prostate—PIN	1/9 (11)	3/9 (33)	5/8 (63)	1/17 (6)	4/17 (24)	6/17 (35)
Prostate—invasive carcinoma: well-differentiated adenocarcinoma					1/17 (6)	1/17 (6)*†
Prostate—invasive carcinoma: undifferentiated	8/9 (89)	6/9 (67)	2/8 (25)*	16/17 (94)	12/17 (71)	9/17 (53)*†
Periaortic lymph node carcinoma	6/7 (86)	1/7 (14)*	2/8 (25)*	8/9 (89)	6/14 (43)*	5/15 (33)*
Lung carcinoma	4/7 (57)	1/7 (14)	1/8 (12.5)	5/9 (56)	5/14 (36)	1/14 (7)*

NOTE: NV1023 or NV1042 (2×10^7 pfu) or virus buffer (mock) was administered systemically on days 0, 3, 7, and 10 in TRAMP mice at either 12 or 18 wk of age. Mice were sacrificed at 24 wk and various tissues were processed for H&E staining and histologically graded. N values are shown in parentheses under each group (s, number of mice sacrificed at 24 wk of age; d, number of mice dead before 24 wk of age).

*P < 0.05, versus mock.

†Combined total of the two types of invasive carcinoma for statistical analysis.

reduction in metastatic frequency in the lungs, it was not significant (Table 1).

To examine whether oncolytic viral therapy could treat metastasis after their onset, TRAMP mice were treated at 18 weeks of age and sacrificed 6 weeks later at 24 weeks (Table 1). A significant reduction in frequency of metastasis to the periaortic lymph nodes was observed with NV1023 (P = 0.04, versus mock, Fisher's exact test) and NV1042 (P = 0.013, versus mock, Fisher's exact test), similar to the observations for treatment at 12 weeks of age. Interestingly, when scored for lung metastasis, a significant reduction was observed in the NV1042-treated mice, with only 1 of 14 (7%) mice exhibiting carcinoma (P = 0.014, versus mock, Fisher's exact test) as compared with 5 of 9 (56%) mock-treated and 5 of 14 (36%) NV1023-treated mice.

Virus biodistribution in NV1042-treated mice. Both NV1023 and NV1042 harbor the *E. coli Lac Z* gene, which acts as a reporter to track these viruses following systemic administration. TRAMP mice treated for 12 weeks with four doses of 2×10^7 pfu of i.v. NV1042 were sacrificed 1, 3, and 7 days after the last treatment, and various tissues (prostate, lung, liver, and brain) were removed for X-gal staining. Results as illustrated in Fig. 4*A* show that 1 day following the final virus injection, X-gal staining was observed in a few isolated cells in the liver and lung and none in the brain (brain data not shown). However, by days 3 and 7, no staining was observed in the lungs, liver, or brain, whereas in the prostate, significant amounts of staining were detected. Thus, systemically administered NV1042 was able to persist at least for 7 days after treatment in the cancerous prostates but not in the normal organs. X-gal staining seen in hyperplastic glands on day 1 was distinct from senescence-associated β-galactosidase (Fig. 4*C*) that has been reported in prostate hyperplasia (27, 28). To further confirm that X-gal histochemistry was identifying LacZ-expressing cells, immunohistochemistry-positive cells were seen in the same region as X-gal–staining cells (Fig. 4*B*).

Biodistribution of NV1042 in 18-week-old TRAMP mice treated systemically on days 0, 3, 7, and 10 was assessed by real-time PCR using HSV *gB* sequences. DNA was isolated from organs (prostate and seminal vesicles, periaortic lymph nodes, lung, liver, brain, and blood) harvested on days 11, 13, and 24. Results shown in Fig. 5 illustrate that viral DNA was detected until day 24 (last day tested) in those organs that harbor primary and metastatic cancers (prostate, periaortic lymph nodes, and lungs). In contrast, whereas many viral copies were detected in the liver and blood on day 1, the level decreased to nondetectable (negative) by day 24, suggesting clearance of virally infected cells or degradation of viral DNA. No viral DNA was detected in the brain of any animal on any day tested.

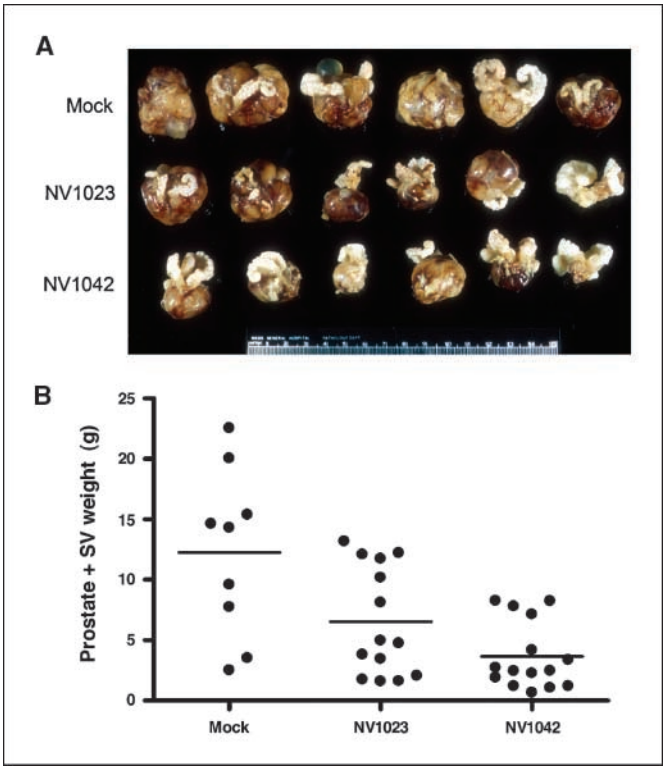

Figure 3. Efficacy of systemic oncolytic virus in TRAMP mice treated at 18 wk of age. *A,* photograph of representative prostate and seminal vesicles excised en bloc from various treatment groups illustrating prostate tumors. *B,* distribution of weights of prostate and seminal vesicles from each treatment group. Mean is denoted by the line in each group; mean weight ± SE for each group are as follows: mock, 12.25 ± 2.3 g; NV1023, 6.54 ± 1.20 g (P = 0.04, versus mock, Mann-Whitney test); NV1023, 3.66 ± 0.72 g (P = 0.002, versus mock, Mann-Whitney test).

Discussion

Prostate cancer in TRAMP mice arises from the targeted expression of SV40 T antigen within the epithelial cells of the prostate (19) and is influenced by the local prostate milieu. Studies using TRAMP mice would therefore be expected to be superior to implanted tumor models for a number of reasons: (*a*) Unlike implanted tumors generated from cultured cells, which are usually of a homogenous clonal phenotype, prostate tumors in TRAMP mice arise multifocally and are heterogeneous in nature, similar to the clinical situation. Such differences make treatment of these multiclonal autochthonous TRAMP tumors more difficult as opposed to implanted tumors. (*b*) Cells grown *in vitro* tend to accumulate additional alterations distinct from the original tumor, potentially influencing the outcome of therapies, thus affecting clinical translation. In contrast, evaluation of autochthonous *in situ* tumors would minimize such external influences. (*c*) *In situ* prostate cancer development as observed in TRAMP mice is a dynamic process between transformed cells and the surrounding stroma and vasculature (29–31), whereas implanted tumors are in an artificial environment with respect to stroma, vasculature, and lymphatic supply, and therefore may respond to therapies more effectively, especially when initiated at a short interval after implantation when the tumor and local stromal cells have not become responsive to one another.

The TRAMP mice used in this study were bred on a FVB/N background. We also attempted to breed the TRAMP mice obtained from The Jackson Laboratory on a C57Bl/6 background, but none of the 250+ F_1 mice advanced from prostate adenoma to carcinoma even at death, which varied from 40 to 52 weeks. This lack of carcinoma development in the C57Bl/6 background is at variance with the original report of TRAMP mice (20) but could be attributed to genetic polymorphisms (32) or dietary and environmental influences (33, 34). Nevertheless, when the F_1 pups from the C57Bl/6 background were crossed with the FVB/N background, the pups from this cross simulated the time line of prostate cancer progression reported previously (35). Even these TRAMP × FVB/N pups exhibited variations in cancer development that differed from previous reports: (*a*) a majority (~75%) of our mice survived only

until 25 weeks as opposed to a previously reported range of 24 to 39 weeks (36); (*b*) none of the 80 mice more than 18 weeks of age displayed bone metastases (20), which may have been due to our inability to detect the occasional incidence of bone metastasis reported in these mice. We also observed some litter/cohort variation, which included (*a*) the rate of penetrance of prostate carcinoma, with some cohorts displaying 100% penetrance whereas others showing less (90%), and (*b*) the survival rate of mice to 24 weeks (as described in the results), with 22% death in the 12-week-old treatment experiment and 47% in the 18-week-old treatment experiment. Such variations highlight the difficulty in conducting treatment studies with spontaneous tumor models, and in fact, most of the literature using TRAMP mice has focused on prevention as opposed to treatment studies (37).

Viruses were administered systemically in this study for several reasons: (*a*) Because we had chosen a regimen of four treatments with the viruses based on our prior studies (17), repeated laparatomies for virus delivery into the prostate would have greatly increased the risk of procedure-related toxicity. (*b*) Systemic administration would be the most effective method to reach various metastatic sites. (*c*) I.v. administration is much more amenable than a surgical procedure from a translational perspective. In this study, NV1042-infected cells were detected within prostate tumors and viral DNA was detected in the cancerous prostates, periaortic lymph nodes, and lungs, suggesting that systemically administered virus reached and persisted in tumor-bearing organs but not in normal organs. Multiple injections of virus did not seem to be toxic, and tumor progression accounted for observed morbidity.

Both NV1023 and NV1042 treatment of TRAMP mice resulted in a significant reduction of primary prostate tumor weight irrespective of the age (12 or 18 weeks) at which treatment was

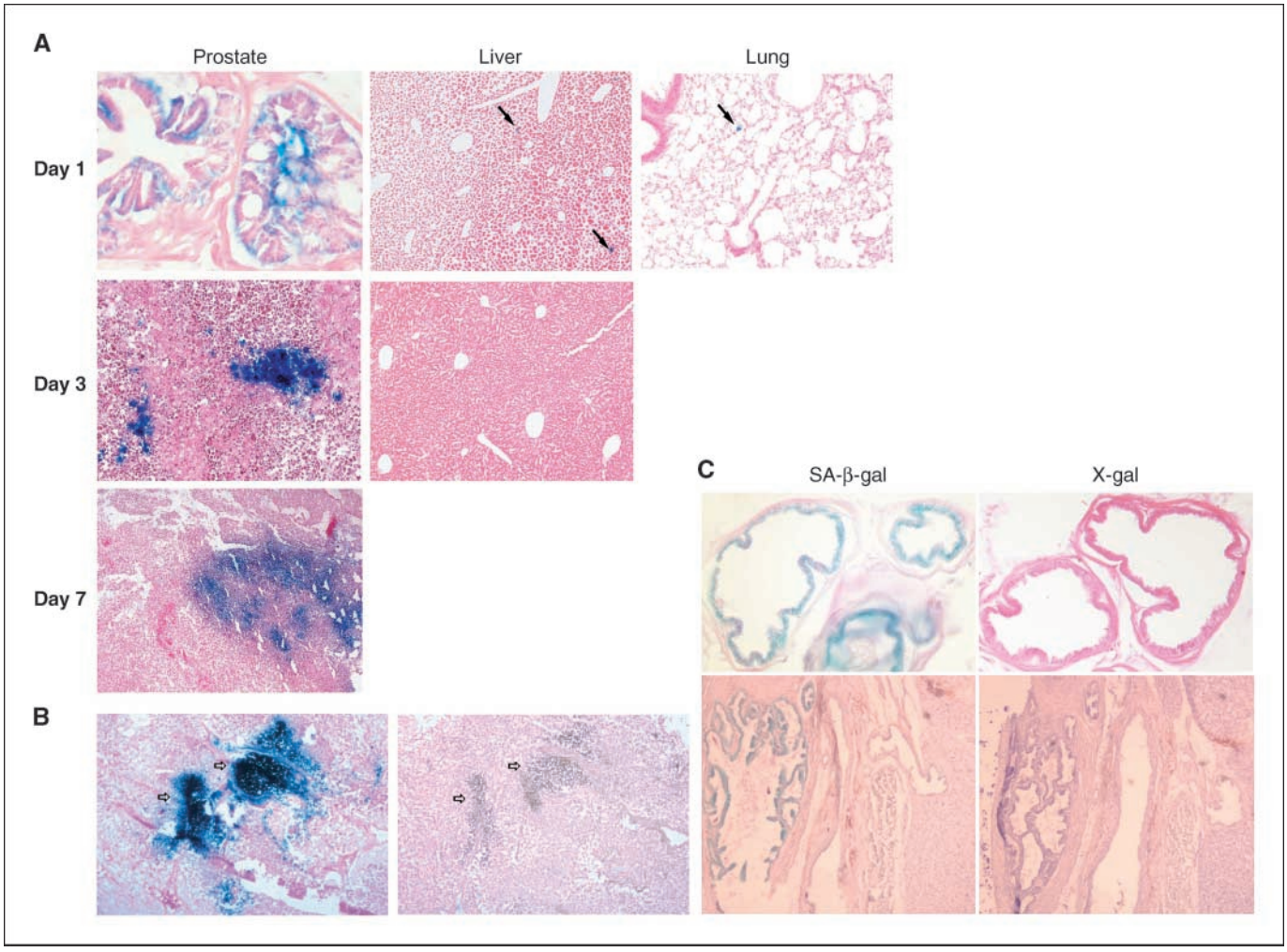

Figure 4. Biodistribution of NV1042 virus following i.v. injection of 12-week-old TRAMP mice. *A,* tissues harvested 1, 3, and 7 d after four viral injections were sectioned and stained with X-gal to detect LacZ expression from the virus. *Top,* sections from prostate, liver, and lungs obtained from mice sacrificed 1 d after treatments showing areas of staining in prostate glands with low-grade PIN and a few X-gal–positive cells in liver and lung (*arrows*); *middle*, tissues from 3 d after virus injections showing X-gal staining in prostate but not in liver; *bottom,* only prostate tissue stained at 7 d after virus injections. *B,* prostate tumor sections from a different mouse at 7 d after virus injections stained with X-gal (*left*) and anti–β-galactosidase antibody (*right*). Note the overlapping LacZ immunohistochemical and X-gal histochemical staining (*open arrowheads*) from nearby sections. *C,* senescence-associated β-galactosidase staining in mock-treated prostate tumors. Frozen prostate sections from a mock-injected TRAMP mouse at 12 wk (as in *A*) were histochemically stained at the same time for senescence-associated β-galactosidase (*SA-β-gal*; *left*) and X-gal (*right*). Cells staining blue are positive. Senescence-associated β-galactosidase was not detected in high-grade PIN or adenocarcinoma. In one mock-treated mouse, small clusters of positive-staining cells were seen in prostate tumors after X-gal histochemistry, likely due to endogenous activity (48).

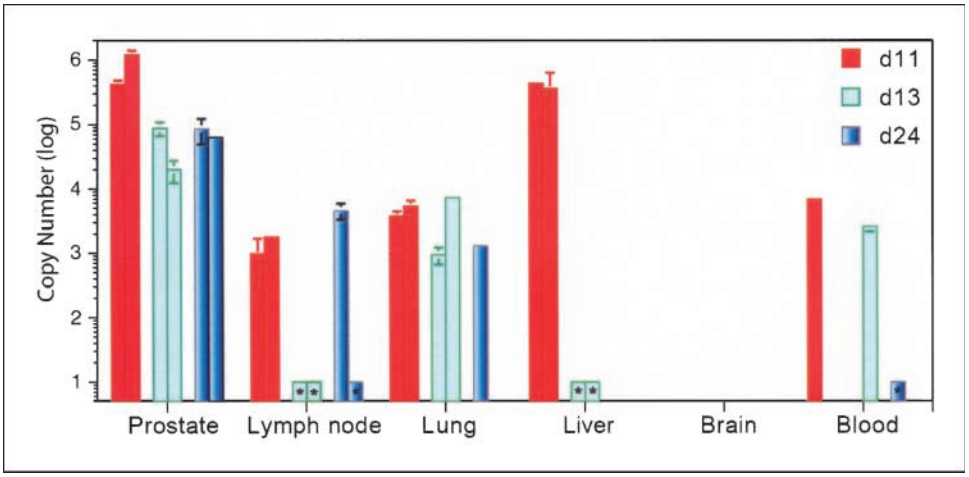

Figure 5. Real-time PCR for HSV gB sequences in various tissues from TRAMP mice treated at 18 wk with oncolytic HSVs. NV1042 (2×10^7 pfu) was administered systemically on days 0, 3, 7, and 10 in TRAMP mice at 18 wk of age and various tissues were harvested on day 11 ($n = 2$), day 13 ($n = 2$), and day 24 ($n = 3$) for absolute quantification of gB viral sequences using TaqMan real-time PCR. Each column represents one mouse. The lymph node is the periaortic lymph node. *, nonquantifiable (1–15 copies). On day 24, there was a third mouse that only had nonquantifiable copies in prostate and periaortic lymph node (not shown in figure). For the second day 24 mouse, no DNA was obtained from the lung, including GAPDH.

initiated; however, only NV1042 was effective in inhibiting the progression from PIN to invasive prostate carcinoma. Both NV1023 and NV1042 also significantly inhibited the frequency of metastasis in periaortic lymph nodes independent of the age (12 or 18 weeks) at which treatment was initiated; however, again, only NV1042 but not NV1023 was significantly effective against metastasis in the lung when treated after the onset of metastasis at 18 weeks of age. Thus, whereas both NV1023 and NV1042 viruses were equally effective against primary tumor growth, only NV1042, and not NV1023, significantly inhibited the progression of primary and metastatic cancer compared with mock. This is an important outcome in determining which virus would be more effective for therapy because mortality in prostate cancer patients is associated with progression to metastatic disease.

We have previously compared the efficacies of NV1042 and NV1023 in s.c. and lung metastatic models using implanted TRAMP-C2 tumor cells and observed varying results, with NV1042 more efficacious in extending survival than NV1023 in the metastatic lung tumor compared with the s.c. model, although the s.c. tumors were directly injected. In the bilateral s.c. tumor model, NV1042 had only a minimal effect on noninoculated tumor growth (17) whereas in the metastatic lung model the enhanced efficacy of NV1042 over NV1023 was abrogated in athymic mice (23). NV1042 has previously been shown to be significantly better than NV1023 at inhibiting tumor growth in squamous cell, hepatic, and colorectal carcinomas (21, 38, 39). Augmented efficacy of IL-12 expression in other oncolytic HSV vectors has also been reported (40, 41).

NV1042 was significantly more effective than mock in the TRAMP mice in almost all of the outcomes measured, whereas NV1023 was only significantly better in less than half. Reasons for the absence of a more significant difference between NV1042 and NV1023 in this study as compared with prior studies (17, 18) include the following: (*a*) Nature of the tumor type: As compared with TRAMP-C2 tumors, the spontaneous TRAMP tumors are multifocal, independently arising in individual glands, and are heterogeneous masses that are continually progressing to more malignant phenotypes with time, along with associated changes in the microenvironment and immune phenotype. (*b*) Exposure of the tumor to IL-12: The *in situ* spontaneous prostate tumors are enclosed within a well-defined capsule, potentially limiting the diffusion of IL-12 expressed from NV1042 virus. (*c*) Less than optimal dosing of the virus: For this highly aggressive spontaneous model, it is possible that more frequent dosing may have increased the differential response between NV1023 and NV1042. (*d*) Timing of efficacy measurement: In the implanted tumor models, efficacy measurements were conducted within a period of 3 to 4 weeks after treatment as compared with 6 to 12 weeks after treatment in the spontaneous tumor model. Such variations in response to the same virus depending on the type of tumor model highlight the importance of evaluating oncolytic viruses in more than one model while emphasizing the need to use models such as the TRAMP mice that are most representative of *in situ* prostate cancer development and progression.

We believe that this is the first report of treating a spontaneous cancer model using systemically administered oncolytic HSVs. We recently reported the intraneoplastic use of oncolytic HSVs in the C3(1)/T-Ag model, which develops mammary tumors spontaneously (42). Although a direct comparison of NV1023 and NV1042 was not conducted, NV1042 significantly delayed mammary tumor progression as compared with mock. Data from both these studies substantiate the utility of NV1042 against spontaneous tumor models, whether administered intraneoplastically or i.v. An IL-12–expressing vector may have some advantages over a noncytokine vector: (*a*) IL-12 binds to receptors on T cells and natural killer (NK) cells, which enhances their proliferation and cytotoxicity, driving a T helper 1 response. It is a central immunoregulator acting as a cross-bridge between innate and adaptive immunity (43) so that when expressed at the site of tumor antigen production, it can boost both arms of the immune response. (*b*) An IL-12–expressing oncolytic virus, which can both cause tumor destruction and deliver an immune-enhancing cytokine in the vicinity of tumor destruction, would be highly beneficial as compared with the direct administration of cytokines into the tumor without sufficient tumor antigens or "danger signals." (*c*) IL-12 also has antiangiogenic properties (44).

Results from multiple studies previously conducted both by us and other investigators to identify the mode of action of NV0142 have also shown consistently without exception that the virus acts through immune and antiangiogenic mechanisms. T cells, specifically $CD8^+$ cells, are essential to the antitumor immune response of the NV1042 virus (17, 23, 38, 45). The role of NK cells seems to vary with the tumor model used; in the metastatic prostate TRAMP-C2 lung tumor model, NK cell activity was observed in mice treated with NV1042 but not NV1023 or virus buffer, whereas in a colorectal micrometastatic model, NK cell depletion did not

interfere with NV1042 efficacy (23, 46). Finally, IL-12 expression by NV1042 virus leads to substantial antiangiogenic activity as shown by the decreased vascularity in prostate and head and neck squamous cell carcinoma models (17, 47).

The current study of systemic HSV treatment in an aggressive spontaneously developing prostate cancer model advances the validity of using oncolytic HSV therapy for prostate cancer patients, especially those with metastatic disease who are severely limited in their treatment options. Importantly, in our study, treatment was initiated not just after primary tumors had developed but also after metastases were apparent, similar to the situation in clinical practice. Given that human cancer cells (including prostate cancer) are more susceptible to HSV oncolysis than mouse cells (ref. 14 versus ref. 17), the TRAMP mouse model serves as a stringent test for efficacy, and it might be expected that the results noted in this animal model could indicate even further efficacy when tested in patients. We have shown that systemically administered oncolytic HSV, in particular the IL-12–expressing NV1042 virus, was effective not only against the primary tumor but also against metastatic tumors independent of their location. These desirable therapeutic features of NV1042 render it a highly valuable agent either as a primary treatment option or as an adjuvant following surgery to eliminate micrometastases.

Acknowledgments

Received 2/19/2007; revised 8/3/2007; accepted 8/14/2007.

Grant support: NIH grant 1R01CA102139-01A1 (R.L. Martuza) and Department of Defense grants DAMD17-98-1-8490 and W81XWH-04-1-0254 (R.L. Martuza) and W81XWH-05-1-0367 (S. Varghese). The real-time PCR core was supported by NIH grant P30 NS045776.

The costs of publication of this article were defrayed in part by the payment of page charges. This article must therefore be hereby marked *advertisement* in accordance with 18 U.S.C. Section 1734 solely to indicate this fact.

We thank Meredith Regan from Dana-Farber/Harvard Cancer Core for assistance with the statistical analyses, Melissa Marinelli and Wenzheng Wang for help with the breeding, Dana Xu and Thanh Thao Huynh for aid in histology, and Luba Zagachin for help in real-time PCR. R.L. Martuza and S.D. Rabkin are consultants to MediGene AG, which provided us with the viruses tested in this study.

References

1. Everts B, van der Poel HG. Replication-selective oncolytic viruses in the treatment of cancer. Cancer Gene Ther 2005;12:141–61.
2. Parato KA, Senger D, Forsyth PA, Bell JC. Recent progress in the battle between oncolytic viruses and tumours. Nat Rev Cancer 2005;5:965–76.
3. Martuza RL, Malick A, Markert JM, Ruffner KL, Coen DM. Experimental therapy of human glioma by means of a genetically engineered virus mutant. Science 1991; 252:854–6.
4. Varghese S, Rabkin SD. Oncolytic herpes simplex virus vectors for cancer virotherapy. Cancer Gene Ther 2002; 9:967–78.
5. Markert JM, Medlock MD, Rabkin SD, et al. Conditionally replicating herpes simplex virus mutant, G207 for the treatment of malignant glioma: results of a phase I trial. Gene Ther 2000;7:867–74.
6. Hu JC, Davis CJ, Graham NJ, et al. Results of a phase I/II clinical trial with Oncovex-GMCSF, a second generation oncolytic herpes simplex virus [abstract]. Am Soc Gene Ther Annual Meeting. 2005.
7. Kuruppu D, Tanabe KK. Viral oncolysis by herpes simplex virus and other viruses. Cancer Biol Ther 2005;4: 524–31.
8. Toda M, Rabkin SD, Kojima H, Martuza RL. Herpes simplex virus as an *in situ* cancer vaccine for the induction of specific anti-tumor immunity. Hum Gene Ther 1999;10:385–93.
9. Thomas DL, Fraser NW. HSV-1 therapy of primary tumors reduces the number of metastases in an immune-competent model of metastatic breast cancer. Mol Ther 2003;8:543–51.
10. Liu BL, Robinson M, Han ZQ, et al. ICP34.5 deleted herpes simplex virus with enhanced oncolytic, immune stimulating, and anti-tumour properties. Gene Ther 2003;10:292–303.
11. Mineta T, Rabkin SD, Yazaki T, Hunter WD, Martuza RL. Attenuated multi-mutated herpes simplex virus-1 for the treatment of malignant gliomas. Nat Med 1995;1: 938–43.
12. Varghese S, Newsome JT, Rabkin SD, et al. Preclinical safety evaluation of G207, a replication-competent herpes simplex virus type 1, inoculated intraprostatically in mice and nonhuman primates. Hum Gene Ther 2001; 12:999–1010.
13. Mashour GA, Moulding HD, Chahlavi A, et al. Therapeutic efficacy of G207 in a novel peripheral nerve sheath tumor model. Exp Neurol 2001;169:64–71.
14. Walker JR, McGeagh KG, Sundaresan P, Jorgensen TJ, Rabkin SD, Martuz RL. Local and systemic therapy of human prostate adenocarcinoma with the conditionally replicating herpes simplex virus vector G207. Hum Gene Ther 1999;10:2237–43.
15. Cozzi PJ, Burke PB, Bhargav A, et al. Oncolytic viral gene therapy for prostate cancer using two attenuated, replication-competent, genetically engineered herpes simplex viruses. Prostate 2002;53:95–100.
16. Fukuhara H, Martuza RL, Rabkin SD, Ito Y, Todo T. Oncolytic herpes simplex virus vector g47δ in combination with androgen ablation for the treatment of human prostate adenocarcinoma. Clin Cancer Res 2005;11: 7886–90.
17. Varghese S, Rabkin SD, Liu R, Nielsen PG, Ipe T, Martuza RL. Enhanced therapeutic efficacy of IL-12, but not GM-CSF, expressing oncolytic herpes simplex virus for transgenic mouse derived prostate cancers. Cancer Gene Ther 2006;13:253–65.
18. Jorgensen TJ, Katz S, Wittmack EK, et al. Ionizing radiation does not alter the antitumor activity of herpes simplex virus vector G207 in subcutaneous tumor models of human and murine prostate cancer. Neoplasia 2001;3: 451–6.
19. Greenberg NM, DeMayo F, Finegold MJ, et al. Prostate cancer in a transgenic mouse. Proc Natl Acad Sci U S A 1995;92:3439–43.
20. Gingrich JR, Barrios RJ, Morton RA, et al. Metastatic prostate cancer in a transgenic mouse. Cancer Res 1996; 56:4096–102.
21. Wong RJ, Patel SG, Kim S, et al. Cytokine gene transfer enhances herpes oncolytic therapy in murine squamous cell carcinoma. Hum Gene Ther 2001;12: 253–65.
22. Meignier B, Longnecker R, Roizman B. *In vivo* behavior of genetically engineered herpes simplex viruses R7017 and R7020: construction and evaluation in rodents. J Infect Dis 1988;158:602–14.
23. Varghese S, Rabkin SD, Nielsen PG, Wang W, Martuza RL. Systemic oncolytic herpes virus therapy of poorly immunogenic prostate cancer metastatic to lung. Clin Cancer Res 2006;12:2919–27.
24. Sambrook J, Fritsch EF, Maniatis T. Molecular cloning: a laboratory manual. Vols. 1 to 3. Cold Spring Harbor (NY): Cold Spring Harbor Laboratory Press; 1989.
25. Shappell SB, Thomas GV, Roberts RL, et al. Prostate pathology of genetically engineered mice: definitions and classification. The consensus report from the Bar Harbor Meeting of the Mouse Models of Human Cancer Consortium Prostate Pathology Committee. Cancer Res 2004;64:2270–305.
26. Dimri GP, Lee X, Basile G, et al. A biomarker that identifies senescent human cells in culture and in aging skin *in vivo*. Proc Natl Acad Sci U S A 1995;92:9363–7.
27. Choi J, Shendrik I, Peacocke M, et al. Expression of senescence-associated β-galactosidase in enlarged prostates from men with benign prostatic hyperplasia. Urology 2000;56:160–6.
28. Castro P, Giri D, Lamb D, Ittmann M. Cellular senescence in the pathogenesis of benign prostatic hyperplasia. Prostate 2003;55:30–8.
29. Condon MS. The role of the stromal microenvironment in prostate cancer. Semin Cancer Biol 2005;15: 132–7.
30. Tuxhorn JA, Ayala GE, Rowley DR. Reactive stroma in prostate cancer progression. J Urol 2001;166:2472–83.
31. Li H, Gerald WL, Benezra R. Utilization of bone marrow-derived endothelial cell precursors in spontaneous prostate tumors varies with tumor grade. Cancer Res 2004;64:6137–43.
32. Asamoto M, Hokaiwado N, Cho YM, Shirai T. Effects of genetic background on prostate and taste bud carcinogenesis due to SV40 T antigen expression under probasin gene promoter control. Carcinogenesis 2002; 23:463–7.
33. Suttie A, Nyska A, Haseman JK, Moser GJ, Hackett TR, Goldsworthy TL. A grading scheme for the assessment of proliferative lesions of the mouse prostate in the TRAMP model. Toxicol Pathol 2003;31:31–8.
34. Suttie AW, Dinse GE, Nyska A, Moser GJ, Goldsworthy TL, Maronpot RR. An investigation of the effects of late-onset dietary restriction on prostate cancer development in the TRAMP mouse. Toxicol Pathol 2005;33: 386–97.
35. Kaplan-Lefko PJ, Chen TM, Ittmann MM, et al. Pathobiology of autochthonous prostate cancer in a pre-clinical transgenic mouse model. Prostate 2003;55:219–37.
36. Hsu CX, Ross BD, Chrisp CE, et al. Longitudinal cohort analysis of lethal prostate cancer progression in transgenic mice. J Urol 1998;160:1500–05.
37. Kasper S, Smith JA, Jr. Genetically modified mice and their use in developing therapeutic strategies for prostate cancer. J Urol 2004;172:12–9.
38. Jarnagin WR, Zager JS, Klimstra D, et al. Neoadjuvant treatment of hepatic malignancy: an oncolytic herpes simplex virus expressing IL-12 effectively treats the parent tumor and protects against recurrence-after resection. Cancer Gene Ther 2003;10:215–23.
39. Bennett JJ, Malhotra S, Wong RJ, et al. Interleukin 12 secretion enhances antitumor efficacy of oncolytic herpes simplex viral therapy for colorectal cancer. Ann Surg 2001;233:819–26.
40. Hellums EK, Markert JM, Parker JN, et al. Increased efficacy of an interleukin-12-secreting herpes simplex virus in a syngeneic intracranial murine glioma model. Neuro-oncol 2005;7:213–24.
41. Parker JN, Gillespie GY, Love CE, Randall S, Whitley RJ, Marker JM. Engineered herpes simplex virus expressing IL-12 in the treatment of experimental

murine brain tumors. Proc Natl Acad Sci U S A 2000;97:2208–13.
42. Liu R, Varghese S, Rabkin SD. Oncolytic herpes simplex virus vector therapy of breast cancer in C3(1)/SV40 T-antigen transgenic mice. Cancer Res 2005;65:1532–40.
43. Trinchieri G. Interleukin-12 and the regulation of innate resistance and adaptive immunity. Nat Rev Immunol 2003;3:133–46.
44. Masiero L, Figg WD, Kohn EC. New anti-angiogenesis agents: review of the clinical experience with carboxyamido-triazole (CAI), thalidomide, TNP-470 and interleukin-12. Angiogenesis 1997;1:23–35.
45. Wong RJ, Chan MK, Yu Z, et al. Effective intravenous therapy of murine pulmonary metastases with an oncolytic herpes virus expressing interleukin 12. Clin Cancer Res 2004;10:251–9.
46. Derubertis BG, Stiles BM, Bhargava A, et al. Cytokine-secreting herpes viral mutants effectively treat tumor in a murine metastatic colorectal liver model by oncolytic and T-cell-dependent mechanisms. Cancer Gene Ther 2007;14:590–7.
47. Wong RJ, Chan MK, Yu Z, et al. Angiogenesis inhibition by an oncolytic herpes virus expressing interleukin 12. Clin Cancer Res 2004;10:4509–16.
48. Weiss DJ, Liggitt D, Clark JG. *In situ* histochemical detection of β-galactosidase activity in lung: assessment of X-Gal reagent in distinguishing lacZ gene expression and endogenous β-galactosidase activity. Hum Gene Ther 1997;8:1545–54.